PERGAMON

Journal of Structural Geology 26 (2004) 271–285

JOURNAL OF STRUCTURAL GEOLOGY

www.elsevier.com/locate/jsg

Maximum effective moment criterion and the origin of low-angle normal faults

Yadong Zheng[a,*], Tao Wang[a], Mingbo Ma[a], Gregory. A. Davis[b]

[a]*The Key Laboratory of Orogenic Belts and Crustal Evolution, Department of Geology, Peking University, Beijing 100871, China*
[b]*Department of Geological Sciences, University of Southern California, Los Angeles, CA 90089-0740, USA*

Received 5 July 2002; received in revised form 2 October 2002; accepted 4 October 2002

Abstract

The origin of the low-angle normal faults of metamorphic core complexes has been debated for over two decades. Proponents of Andersonian fault mechanics have long argued that it is mechanically unfeasible for slip to occur along shallowly dipping normal faults. A new theory, named the maximum effective moment criterion, is proposed here for their origin. Using an effective moment approach formulated as $M_{\text{eff}} = FH$, where F is the force tangentially acting on the unit shear boundaries and H represents its arm. The maximum value appears at angles of $\pm 54.7°$ with the σ_1. Since extensional crenulation cleavages (eccs) and the contractional crenulation cleavages (cccs) occur in conjugate pairs with $\sim 110°$ angle between them, it is suggested that they tend to be oriented in the directions of maximum effective moment. The differential stress for formation of the ecc or ccc are less than that for fracturing. The orientations of conjugate eccs depending on relative magnitudes of simple shear versus coaxial strain components. The synthetic ecc set is much better developed than the antithetic set due to anisotropy. Upward propagation of the synthetic ecc set from mid-crustal domains of mylonitization through strain localization and strain softening is considered an effective mechanism for the formation of the low angle-normal faults of metamorphic core complexes. Published by Elsevier Science Ltd.

Keywords: Low-angle normal fault; Extensional crenulation cleavage; Maximum effective moment criterion

1. Introduction

Since recognition of low-angle normal or detachment faults in western North American metamorphic core complexes (e.g. Davis and Coney, 1979; Crittenden et al., 1980; Wernicke, 1981; Lister and Davis, 1989), the mechanics of their formation has stimulated great interest. Similar faults have subsequently been reported elsewhere in the world (e.g. Lister et al., 1984; Doser, 1987; Abers, 1991; Zheng et al., 1991; Davis et al., 1996, 2002; Boncio et al., 2000; Sorel, 2000). Their origin has conflicted with classic Andersonian theory (Anderson, 1951), which predicts that normal faults can only form with dips higher than 45°. Formation of low-angle normal faults, according to such a theory, requires the principal stress axes in the brittle upper crust to be significantly inclined with respect to the earth's surface. Elastic models with shear tractions applied to the base of the upper-crustal brittle layer were proposed by Yin (1989) as providing a possible cause of inclined principal stress axes. Buck (1990) and Wills and Buck (1997), however, claimed that shear tractions applied to the brittle layer cannot be greater than ~100 MPa and could not, therefore, initiate low-angle normal faulting. Westaway (1999) later presented model stress fields to show that appropriately oriented stress fields could be generated at the base of the brittle layer, but only if shear tractions locally reach ~100 MPa. However, such tractions are only possible under extreme conditions requiring dramatic lateral variations in the state of stress across an extending region.

All of these analyses are based on elastic modeling of stress fields within the crust and the Coulomb–Mohr failure criterion with an angle of internal friction of ~30° (corresponding to a coefficient of friction of 0.5). Based on Byerlee's law (Byerlee, 1978), the coefficient of friction is independent of rock type and depends solely on values of shear and normal stress. This suggests that the angle of internal friction should change with depth. However, even if the coefficient of friction were zero, Byerlee's law would not be applicable to the mechanism for generating low-angle

* Corresponding author. Fax: +86-10-6275-1187.
E-mail address: ydzheng@pku.edu.cn (Y. Zheng).

0191-8141/03/$ - see front matter Published by Elsevier Science Ltd.
doi:10.1016/S0191-8141(03)00079-8

normal faults. The fact that the low-angle normal faults of metamorphic core complexes are associated with ductile shear zones may provide a clue to the mystery, and this fundamental observation appears to have been neglected. The aim of this article is to assess the mechanism (s) of development of low-angle normal faults based on insights into the evolution of ductile shear zones. This discussion is not concerned with the deeper, low-angle geometry of listric normal faults, which are common in the brittle regime (Price and Cosgrove, 1990). What we try to explain here are low-angle normal faults that we propose are generated as extensional crenulation cleavages within ductile shear zones.

2. Previous studies

2.1. Conjugate angle of crenulation cleavages

A crenulation cleavage is a spaced cleavage that forms when an earlier foliation has been deflected into a new orientation, forming a series of straight-limb-dominant, small folds with narrow, tight curved hinges. Price and Cosgrove (1990) pointed out that when a layering is contracted parallel to the foliation, conjugate reverse kink-bands may form, and when compressed normal to the foliation, conjugate normal kink-bands may form (Fig. 1). Some authors (e.g. Platt and Vissers, 1980; Passchier, 1991) used the terms compressional crenulation cleavage (ccc) and extensional crenulation cleavage (ecc) for these two types of cleavage. Although cccs are not relevant to low-angle normal fault development, both ccc and ecc have the same conjugate angle and both are controlled by the maximum effective moment criterion (see Section 3 for reasons). As important evidence for the maximum effective moment criterion, conjugate angles of natural and experimental observations of cccs are included in Table 1. In both situations, the maximum principal compressive stress bisects the obtuse angle. The conjugate angle is usually ~110° in the direction of maximum shortening, suggesting ecc and ccc have something in common (Table 1). For the

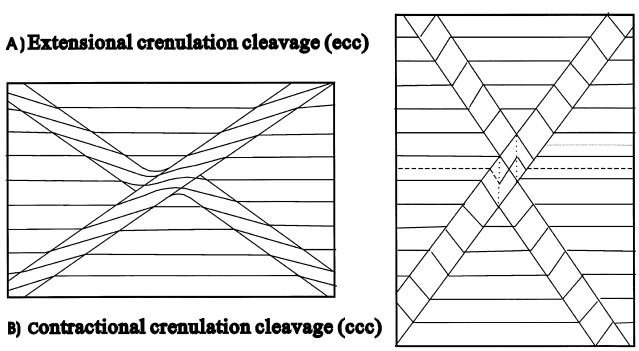

Fig. 1. Conjugate ecc (A) and ecc sets (B). The obtuse conjugate angle containing the shortening direction or the referred σ_1.

present study, however, attention is here confined to the extensional crenulation cleavage in ductile shear zones.

Ductile shear zones often contain a penetrative foliation that is sigmoidal with respect to discrete sub-parallel minor shear bands. The shear bands transect and displace the penetrative mylonitic foliation at a small angle, which implies that they formed during relatively later increments of a progressive deformation (Fig. 2A). The latter are variably termed shear-band cleavages (White, 1979; Gapais and White, 1982; Passchier, 1991), C′-surfaces (Berthe et al., 1979), extensional crenulation cleavages (Platt, 1979; Passchier, 1991), normal kink-bands (Price and Cosgrove, 1990) or normal-slip crenulations (Dennis and Secor, 1987), and flanking shear bands (Passchier, 2001). Since shear-band foliations superficially resemble a crenulation cleavage but are developed by extension of the older foliation rather than shortening, they are sometimes referred to as extensional crenulation cleavages (eccs) or normal-slip crenulations. White (1979) shows conjugate shear bands intersecting and symmetrically disposed about the mylonite foliation at ~35°, an angular relationship commonly reported in both field studies and laboratories (Table 1). The conjugate shear band angle, therefore, is ~110°.

Several theories for the origin and evolution of the planar fabrics in shear zones have been proposed. Platt and Vissers (1980) suggested that eccs might be comparable with slip lines in plastic material (Hill, 1950). Since slip lines would follow the characteristic directions of the flow field, they would be oriented normal and parallel to the shear plane of simple shear. The two sets of ecc, however, are commonly oblique to the slip plane, with the dominant synthetic set at a small angle to the shear zone boundaries. Subsequently, Platt (1984) suggested that two possible reasons for this obliquity are (A) the cleavage zones do not propagate parallel to a characteristic direction of the flow field, or (B) the flow field deviates from overall simple shear due to flow partitioning. He preferred the second possibility, as it may also provide an explanation for the deformation of conjugate and multiple ecc sets. In his model, conjugate ecc sets form at 45° to the foliation, which does not correspond well with observations in natural shear zones (e.g. Fig. 2 and Table 1).

Simpson and De Paor (1993) suggested a possible association between the orientation of eccs and the directions of maximum shear strain rate and not with the flow apophysis directions. If this theory were applicable to shear bands the conjugate pairs should be normal to each other. Blenkinsop and Treloar (1995) proposed that C′-surfaces form in the orientation of a Coulomb failure surface at an angle of less than 45° to the maximum principal stress. If the crenulation cleavages were the result of 'brittle' shear failure, then the angle between the conjugate cleavage planes should be less than 90°. However, in all the cases shown in Fig. 1 and Table 1, the angle between the conjugate cleavage planes exceeds 90°. Knill once suggested (see refs in Price and Cosgrove, 1990) that this angle was originally less than 90° and that

Table 1
Natural (N) and experimental (E) conjugate angles of contractional crenulation cleavage (ccc) and extensional crenulation cleavage (ecc) pairs

N/E	Ccc	Ecc	References
E	110–130°		Paterson and Weiss, 1966; Weiss, 1968
E	~115°		Gay and Weiss, 1974
E	~115°		J. Asselin, 1975 (Fig. 12.29 in Price and Cosgrove, 1990)
E	130°		Fig. 13.28(b) in Price and Cosgrove, 1990
N	~120°		Paterson and Weiss, 1966; Weiss, 1968
N/E	110–120°		Anderson, 1964, 1974
N	105–109°		Hobbs et al., 1976
N	101–118°		Roberts (cf. Johnson, 1977)
E	110.8°		Friedman and Logan, 1973
E	~110°	~110°	Cosgrove, 1976
N		110°	Platt and Vissers, 1980
N		109°	Park, 1981
E		100°	Peltzer, 1983 in Harris and Cobbold, 1985
N/E		~120/95–104°	Harris and Cobbold, 1985
E		105–107°	Wolderkidan (Fig. 16.11(c) in Price and Cosgrove, 1990)
N		~110°	White, 1979; White et al., 1980
N		100–110°	Halbich, 1978
N		~110°	White, 1979; White et al., 1980
N		~120°	Zhang et al., 1998
N		110°	Wang et al., 2002b

subsequent flattening had increased the angle to more than 90°. The experimental study on kink bands by Paterson and Weiss (1966), however, shows that the initial angle is and remains ~120° until 30% shortening. Price and Cosgrove (1990) summed up the relationship between the conjugate crenulation cleavage and the slaty cleavage in the Dalradian phyllites of Cragnish, Argyllshire. They pointed out that in most of the examples measured in the area, the σ_1 axis bisects the obtuse angle between crenulation cleavages and, therefore, suggests that the conjugate crenulation cleavage in the area is the result of the formation of normal kink-like structures and not of the subsequent flattening of conjugate faults formed by satisfying the criteria for brittle shear failure. Using a moment approach, Hoeppener et al. (1983) and Zheng and Du (1985) analyzed the angle between conjugate kink bands (contractional crenulation cleavages or cccs) and determined a theoretical dihedral angle of 54.7° about the maximum principal compressive stress axis (σ_1). Subsequently, Zheng (1992) suggested that this angle is also suitable for conjugate ecc sets (see Section 3 for reason). This theoretical deduction agrees well with both field and experimental observations (Table 1).

Watterson (1999) re-evaluated the theory of Becker (1893) and proposes the concept of failure along zero extension directions and predicts, with isovolumetric strain, yield occurs on plans at 45° to the principal shortening direction in plane strain and at 54.7° to this axis in uniaxial shortening. The latter prediction is intriguing, for the value is exactly the same as suggested in this study (see Section 3). Unfortunately, the value is only applicable to uniaxial shortening, and the locus of zero extension directions of the bulk strain that he predicts is everywhere at 54.7° to the *Z*-axis, i.e. the locus of zero extension directions should be a conical surface rather than a plane.

It is surprising and puzzling that the angle of 54.7° coincides with the result under mono-axial extensional cases in the mathematical theory of plasticity, for the conclusion derived from slip line theory is that the maximum principal stress bisects the *acute*angle rather than the obtuse one of conjugate slip line sets (Hill, 1950). This implies that the slip line theory is not directly applicable to shear bands.

2.2. Preferential development of a synthetic ecc set due to anisotropy

Since the contraction orientation or the compressive stress axis (σ_1) is commonly oblique to the pre-existing foliation, conjugate ecc or ccc sets, therefore, are not necessarily symmetrically disposed about the mylonite foliation except for coaxial deformation (Fig. 2D). Although conjugate ecc sets occasionally occur in shear zones (Bergh and Karlstrom, 1992; Hetzel et al., 1995; Goodwin and Williams, 1996; Argles et al., 1999), many workers have noted that synthetic eccs or C′ are usually much better developed than antithetic ones (Fig. 2A and B). The reason is probably the anisotropy of mylonitic rocks. Donath's experimental study (1961, 1964, 1968) is very relevant in this regard. By loading to failure a series of cylinders of slate cut at different angles, a varied relationship between attitude of the shear fracture plane and slaty cleavage was found. Conjugate fractures were obtained in only two situations: slaty cleavage parallel and perpendicular to the long axis of the cylinder. In these two configurations the slate is effectively isotropic. In all others only one fracture

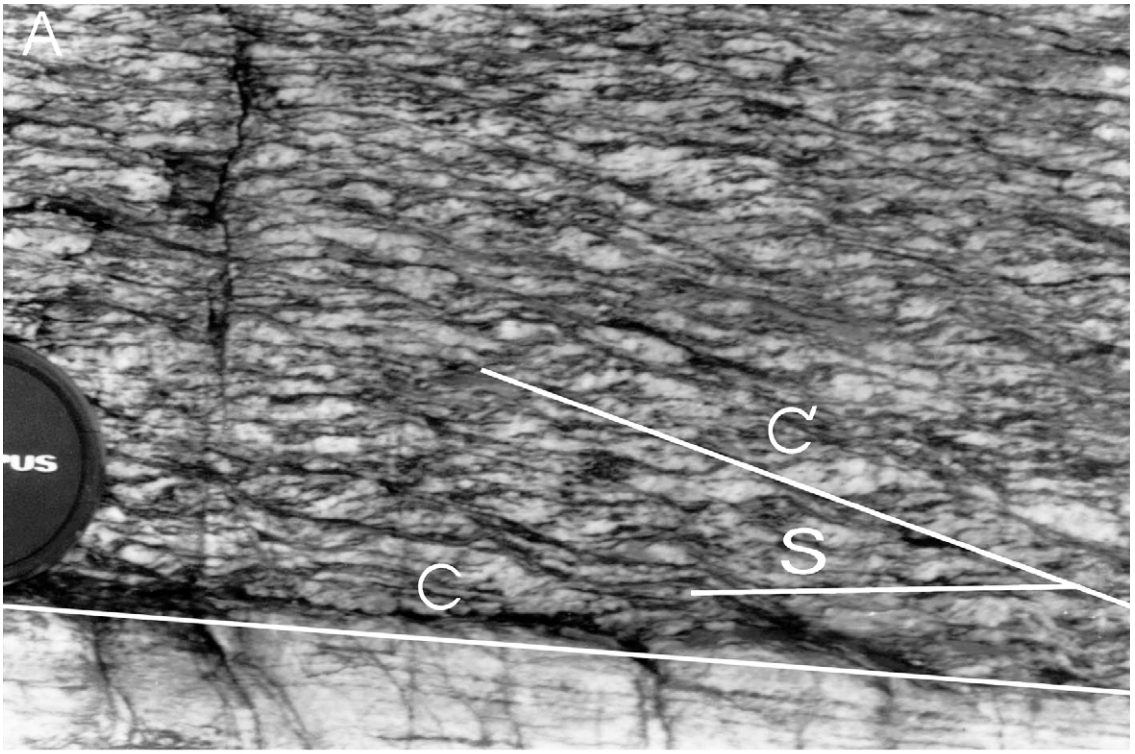

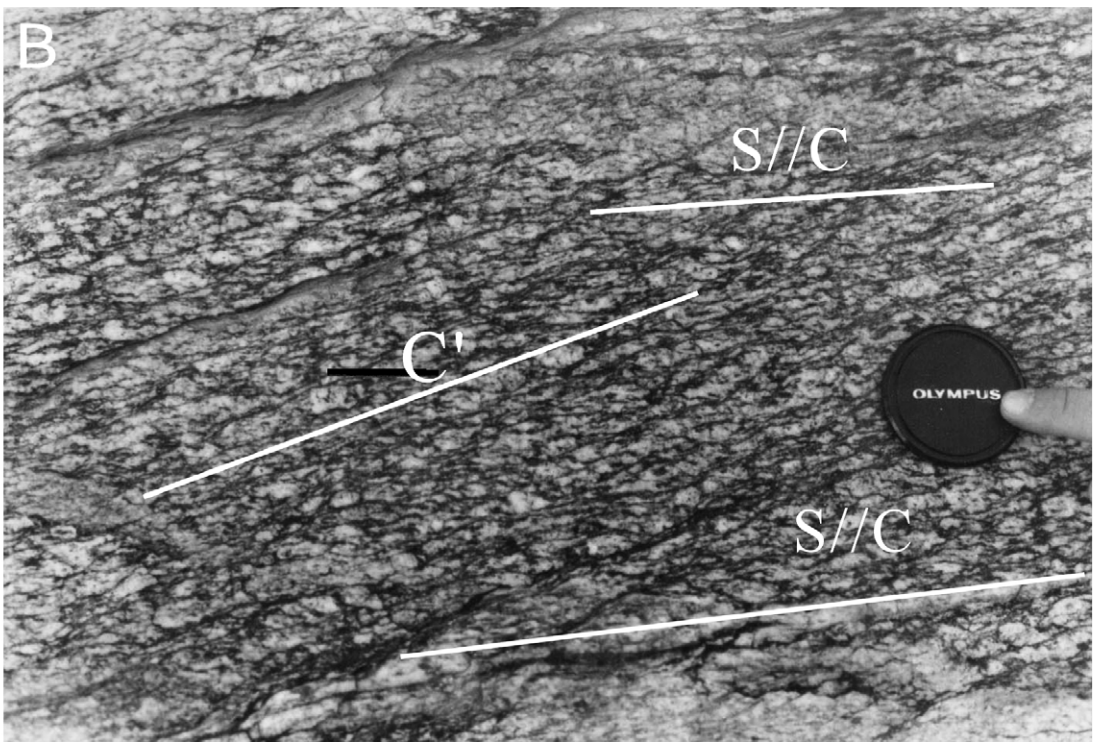

Fig. 2. Outcrop-scale synthetic ecc or C′ in the Yagan metamorphic core complex (A) and some that have turned into small low-angle normal faults (B). Outcrop-scale conjugate ecc sets with an obtuse angle (120°) to the shortening direction in the Yagan metamorphic core complex (C) and micro-conjugate ecc sets with an obtuse angle (110°) in the Hohhot metamorphic complex, Inner Mongolia (D): Mus—muscovite; Pl—plagioclase. The outcrop surfaces and thin section are sub-parallel to the lineation and normal to the foliation in the rocks.

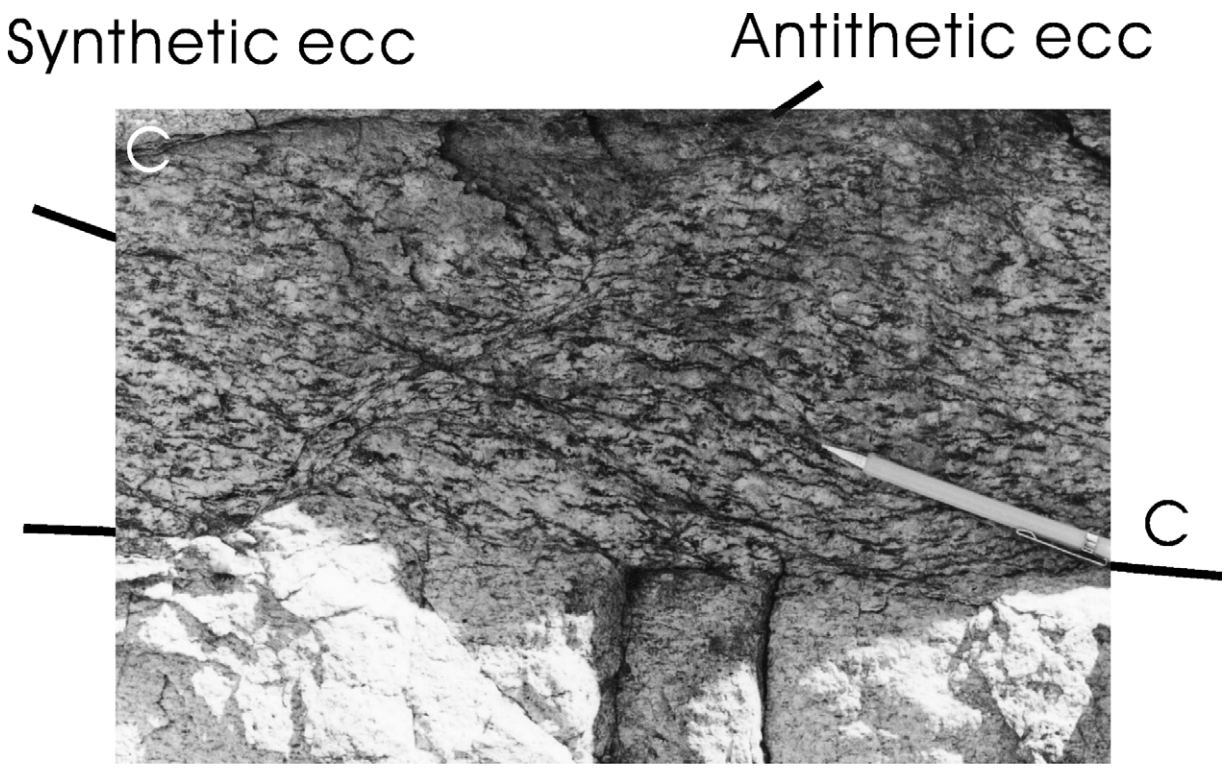

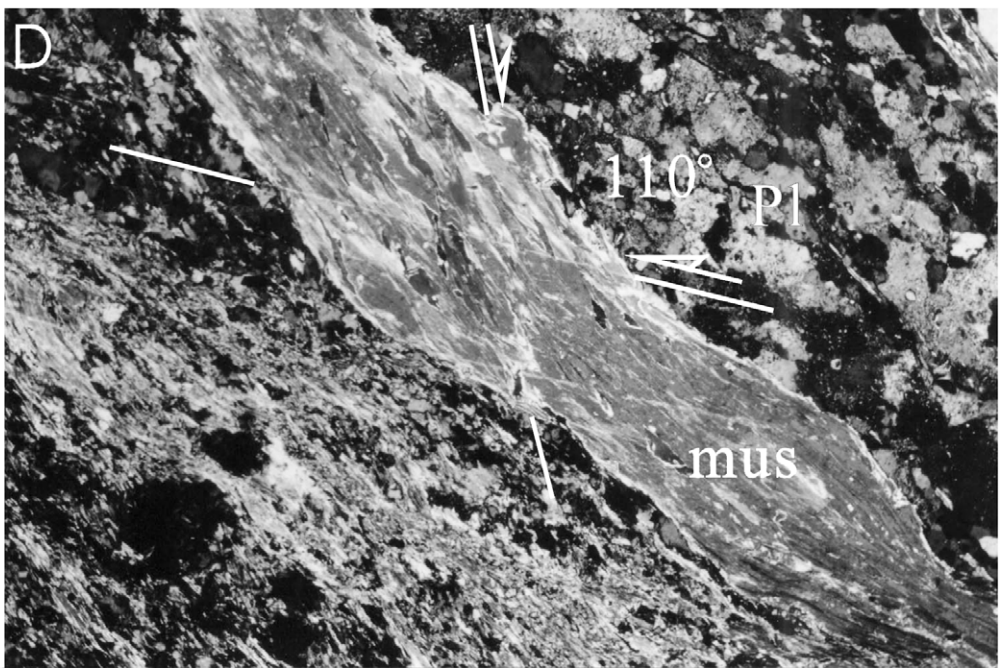

Fig. 2 (*continued*)

developed, and its attitude was controlled, either directly or indirectly, by the slaty cleavage. More recently, Shea and Kronenberg (1993), based on their experiments on foliated rocks, demonstrated the strong influence of anisotropy on the strength of foliated rocks: compressive strengths at 90° to the foliation are over four times higher than at 45° under the conditions tested ($T = 25\,^{\circ}C$, $P_c = 200$ MPa and $\dot{\varepsilon} = 10^{-5}\,s^{-1}$). It is expected that the shear strength of foliated rocks at low angles to foliation is much less than that at high angles to it. In coaxial deformation (e.g. pure shear), the conjugate ecc sets are equivalent in strength, whereas in non-coaxial deformation (simple shear and general shear cases), foliated rocks are much weaker in the synthetic than in the antithetic ecc orientation. Obviously, a synthetic ecc set is mechanically preferable; the antithetic set cannot develop before the resolved shear stress on the surface is raised to a value high enough to cause its initiation. Based on an experimental study of artificial KCL-mica schist, Williams and Price (1990) concluded that conjugate shear bands develop in the case of S-foliation-normal shortening and single shear-bands occur in the case of S-foliation-parallel shear. This lends additional support to the strong influence of anisotropic strength of foliated rocks on the formation of ecc sets.

2.3. Range of angles between ecc and mylonitic foliation

The angle between the synthetic ecc and shear zone boundaries proposed by various authors generally ranges from 15 to 35°, but has been reported as high as 45° (Passchier and Trouw, 1996). Weijermars (1993, 1998) has discussed in detail the theoretical relationship between flow patterns, the stress orientation and the direction of boundary displacement. It is shown that in two-dimensional thinned shear zones, the angle between the maximum principal stress σ_1 and the shear plane or the mylonitic foliation at some high finite strains (e.g. shear strain [γ] more than 10) may range from 45 to 90° depending on the related kinematic vorticity number (W_k), i.e. relative magnitudes of simple shear versus coaxial strain components. For pure shear cases ($W_k = 0$), the angle between the maximum principal stress σ_1 and the shear plane is 90°, whereas for simple shear cases ($W_k = 1$), the angle is 45°. The limiting assumptions that Weijermas made are: (1) homogeneous bulk deformation; (2) no volume changes; and (3) plane deformation. Even an assumption of steady-state flow is not required if only the ratio of the vorticity and strain rate remain fixed (Weijermars, 1998).Since the conjugate angle of ecc sets is ~110° and the angle between the inferred σ_1 and the cleavage is ~55°, the crenulation cleavage orientation with respect to the mylonitic foliation for pure shear is ±35° and synthetic crenulation cleavage is −10° (45–55°) for simple shear. Note that the negative value, measured anti-clockwise from the shear zone boundary, shows that the synthetic cleavage for simple shear may form as a synthetic ccc set or flanking folds (Passchier, 2001) rather than ecc (Fig. 3). The ccc set for simple shear and simple shear-dominated shear may lead to the formation of small-scale thrusts or flanking folds, which have a similar orientation to *p*-shears in brittle shear zones (Tchalenko, 1968). Evans and Dresden (1991) have noted the geometrical similarity between shear surfaces in 'brittle fault zones' and S–C mylonites. Obviously, neither a synthetic ecc nor a ccc slip system can develop precisely parallel or sub-parallel to the mylonitic foliation. Slip will probably occur on mylonitic foliation surfaces before the resolved shear stress on them is raised to a high enough value to cause initiation of a new slip surface.

3. Maximum effective moment criterion

Ecc and ccc surfaces develop in foliated rocks; the essential features of conjugate ecc sets are shown in Fig. 1. Since the foliation within the crenulation cleavage zones is rotated with respect to the foliation outside the zones, the foliation rotation must result from forces tangentially acting on the cleavage boundaries. Following conventional practice, a unit square cut from a potential cleavage zone whose foliation has not yet rotated is taken to analyze the stress state as shown in Fig. 4. The normal stress σ_θ and the shear stress τ_θ acting on cleavage boundaries are given respectively by:

$$\sigma_\theta = \frac{1}{2}(\sigma_1 + \sigma_3) + \frac{1}{2}(\sigma_1 - \sigma_3)\cos 2\theta$$

and

$$\tau_\theta = \frac{1}{2}(\sigma_1 - \sigma_3)\sin 2\theta \quad (1)$$

$$= -\frac{1}{2}(\sigma_1 - \sigma_3)\sin 2\alpha \quad (2)$$

where σ_1 and σ_3 are the maximum and minimum principal stresses, θ is the angle between σ_1 and the normal to the cleavage and α is the angle between σ_1 and the cleavage itself. Eq. (2) means that the shear stresses acting on the two orthogonal surfaces are equal in absolute value but opposite in sense (Fig. 4B). The system is in equilibrium, i.e. the sums of the forces and moment are zero and the cube neither accelerates nor rotates. To create a deformation band, however, there must be an effective moment M_{eff} that drives the foliation in the cleavage zone to rotate away from its initial orientation in the same sense. The effective moment (M_{eff}) driving the foliation to rotate is given by the force (F) tangentially acting on the boundaries of the potential cleavage and its arm H:

$$M_{eff} = FH$$

Since F = stress × area A, the stress is equivalent to the force if we substitute the stress for the force acting on the side of a unit area. The force is an effective shear stress τ_{eff}.

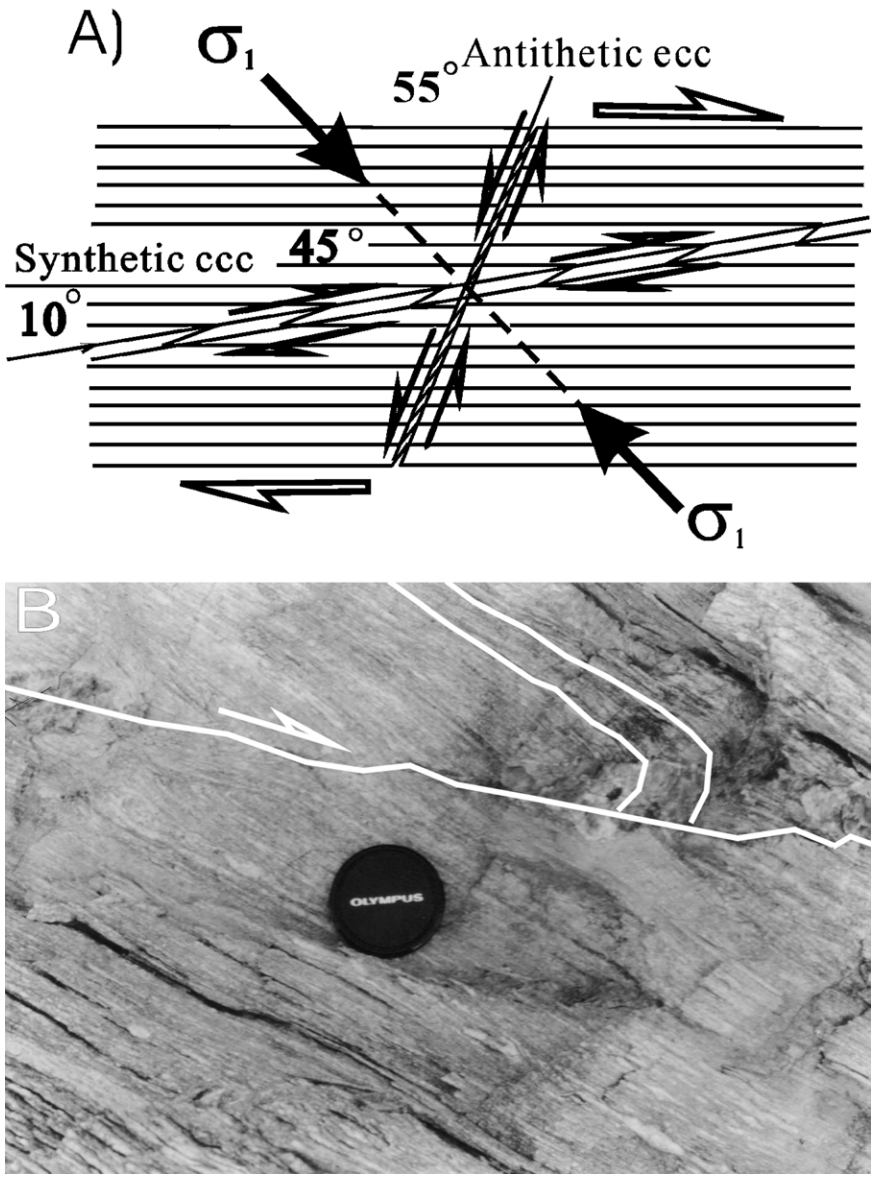

Fig. 3. (A) Based on the conjugate angle of 110° bisected by principal shortening, the synthetic crenulation cleavage orientation is − 10° (45–55°) for simple shear at some high finite strain (γ more than 10). Note that the negative value, measured anti-clockwise from the shear zone boundary, shows that the synthetic cleavage may form as synthetic ccc or flanking folds rather than ecc. (B) A ccc or small-scale thrust on the southern flank of the Yagan-Onch Hayrhan metamorphic core complex. The lineation on the thrust surface is sub-parallel to that on the mylonitic foliation and is interpreted to mean that the main foliation and the thrust belong to the same progressive deformation history.

Therefore:

$$M_{\text{eff}} = \tau_{\text{eff}} H = \tau_{\theta} L \sin\alpha \tag{3}$$

where L is the side of the unit square or $H_{\max}$ in the σ_1 direction (Fig. 4A). Substituting Eq. (2) into Eq. (3), then becomes:

$$M_{\text{eff}} = \frac{1}{2}(\sigma_1 - \sigma_3) L \sin 2\alpha \sin\alpha \tag{4}$$

Relationship (4) demonstrates that the effective moment is only a function of the differential stress and the orientation of the cleavage with respect to the σ_1 direction. Given a value of the differential stress for a certain material, the maximum value of the effective moment appears in the orientation of − 54.7° as shown in Fig. 5. This relationship is here named the maximum effective moment criterion. In a similar analysis of kink zones by Hoeppener et al. (1983), Eq. (4) was termed the effective shear stress. However, the physical implication of the equation is an effective moment rather than an effective shear stress.

Since Eq. (4) only involves α and is independent of the deformed material and the orientation of foliation, this relationship holds for any rock or material that contains a pre-existing well developed foliation (bedding, cleavage, or schistosity) (see Anderson, 1964; Dewey, 1965; Weiss, 1980)

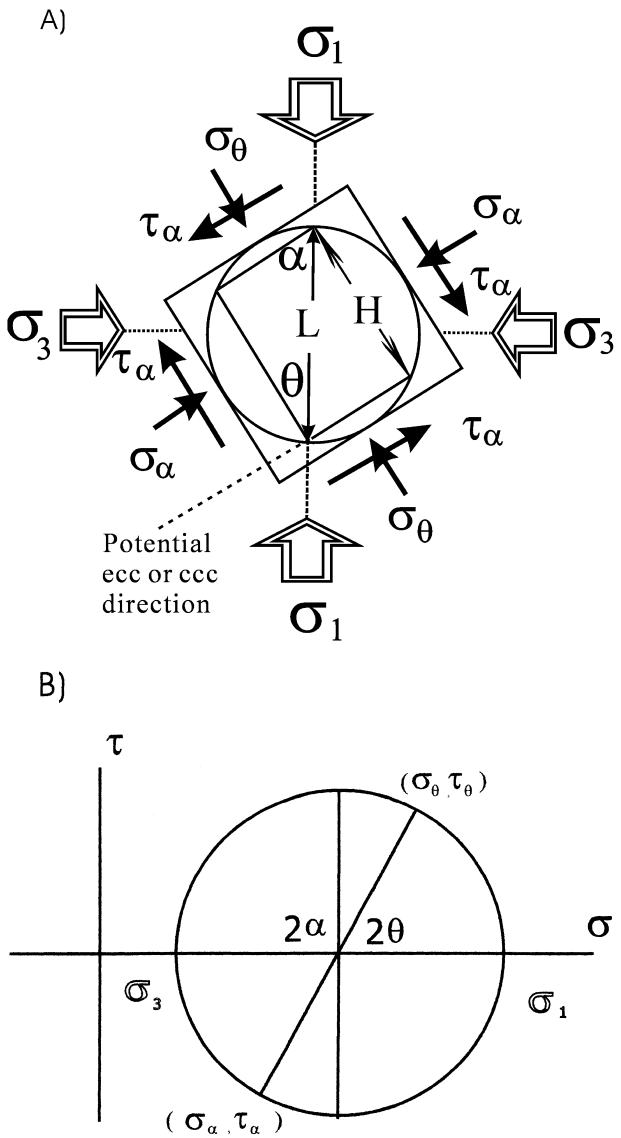

Fig. 4. Stress state on the boundary of a unit block of ecc (A) and its Mohr stress circle (B). σ_1 and σ_3—the maximum and minimum principal stresses; θ—the angle between σ_1 and the normal to the cleavage; α—the angle between σ_1 and the cleavage itself; H—arm; L—the side of the unit cube or H_{max} in the σ_1 direction.

and regardless of the angle between σ_1 and the foliation. The result, therefore, is not only applicable to the development of eccs but also to cccs. In both situations, the maximum principal compressive stress bisects the obtuse angle between the crenulation cleavages. However, the former are features usually developed in rocks from ductile shear zones (e.g. Mamtani and Karanth, 1996), while the latter occur in both ductile and brittle environments (e.g. Paterson and Weiss, 1966; Donath, 1968; Weiss, 1968, 1980; Shea and Kronenberg, 1993). Since both cases involve foliation or layering of rocks, strong anisotropy of materials seems necessary for ecc and ccc formation. Price and Cosgrove (1990) have shown the difference between eccs and cccs: the layering inside the

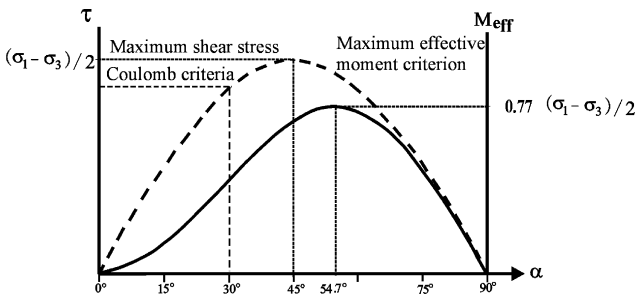

Fig. 5. Relationship between differential stress, shear stress and effective moment showing the maximum effective moment at 54.7° direction with σ_1. There is no remarkable M_{eff} drop from the maximum value within the range of 54.7 ± 10° and the range of 45–65° with σ_1 is favorable for the formation of both ecc and ccc.

ecc is always thinner than that outside and must continue thinning as the structure amplifies, whereas the layering inside a kink band must separate or thicken during initial rotation. The change in thickness is much more easily accomplished in ductile regimes than in brittle ones. Thus, there seems to be a competition between mechanisms of kinking and frictional fracturing in brittle regimes. Whether the rock kinks or fractures depends on which criterion (the Coulomb–Mohr failure criterion or the maximum effective moment criterion) is more easily satisfied. It is worthy to notice that the differential stress for formation of the ecc or ccc are less than that for fracturing as shown in Fig. 5. The maximum effective moment criterion in ductile and brittle regimes seems to be equivalent to the Coulomb–Mohr criterion in the brittle regime; the maximum effective moment and the Coulomb–Mohr criterion constrain the orientations of crenulation cleavages and frictional fractures, respectively.

The above analysis shows that the conjugate angle of crenulation cleavages bisected by σ_1 is 2α, i.e. 109.4°, which is almost the same as the value suggested by White (1979). The M_{eff} curve in Fig. 5 shows that there is no remarkable M_{eff} drop from the maximum values within the range of 54.7 ± 10°. The range is favorable for the formation of both eccs and cccs and covers all the natural and experimental examples shown in Table 1.

4. Relationship between eccs and low-angle normal faults

4.1. The Yagan-Onch Hayrhan metamorphic core complex

The complex is exposed on the Sino-Mongolian border (Zheng et al., 1991; Webb et al., 1999) as an ENE-trending, elliptical dome-like outcrop of quartzo-feldspathic mylonitic rocks and gneisses cut by plutons and bounded above by the Hure detachment fault (Fig. 6). Below the detachment is an ~1.5-km-thick section of mylonitic rocks. Mylonitic

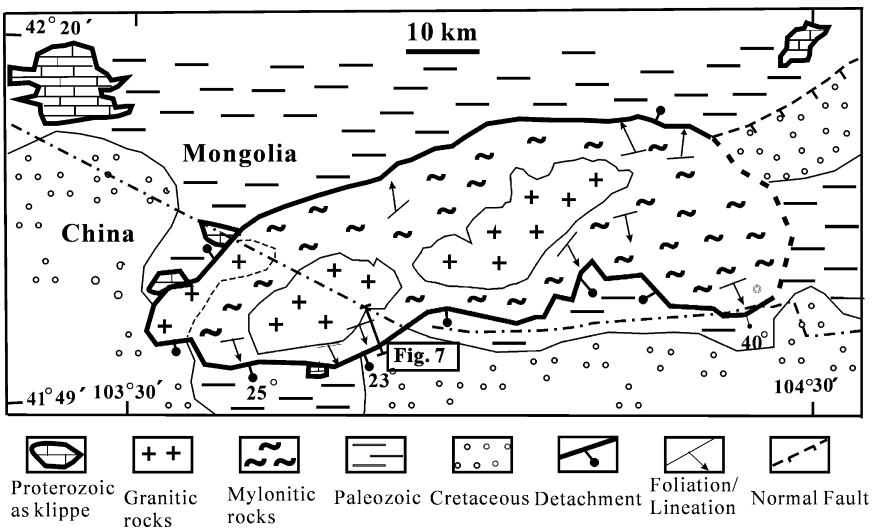

Fig. 6. Simplified geological map of the Yagan-Onch Hayrhan metamorphic core complex.

foliation in the footwall rocks defines the dome structure and dips gently outwards, and stretching lineations defined by quartz, biotite, and feldspar plunge mainly south-southeast, or partially north-northwest. The hanging wall consists of low-grade Paleozoic and unmetamorphosed Mesozoic sedimentary and volcanic rocks. A number of ages ranging from 171 to 129 Ma have been determined for the syn-kinematic granites and mylonites from the core complex (Zheng et al., 1991; Zheng and Zhang, 1994; Webb et al., 1999; Wang et al., 2002a).

Since shear sense here is consistently top-to-the-south-southeast, the southern flank of the core complex is the normal one that shows a top-to-down-dip relative displacement. A ~4-km-long section across the southern flank of the core complex region is selected to study in detail the structures in the footwall mylonitic rocks and the detachment itself (Fig. 7).

4.2. Fabrics in the footwall mylonitic rocks

The most obvious feature in the mylonitic rocks is a penetrative mylonitic foliation that is defined by a planar compositional layering and a lineation. It commonly contains elongate and asymmetric feldspar porphyroclasts. The foliation in the matrix wrapping around the elongate porphyroclasts shows a smooth change in orientation, giving rise to a typical sigmoidal pattern, which is oblique adjacent to center of porphyroclasts and curved into the over-all foliation at the ends of the porphyroclast tails. Both σ- and δ-type porphyroclast systems and other markers indicate top-to-the-south-southeast (Zheng et al., 1991; Zheng and Zhang, 1994; Wang et al., 2002a). Based on 51 measurements in the section, the mylonitic foliation has a dip and dip direction of 6 to 166° and the stretching lineation is oriented downdip.

A synthetic ecc set or C′ is well developed in the mylonitic rocks. These features are small, subparallel, evenly spaced at 1–10-cm intervals and deflect or cut the mylonitic foliation (Fig. 2A and B). The compositional layering is thinned, and richer in biotite in the ecc set and the mylonitic fabric is stronger than in the adjoining mylonitic rocks. The synthetic ecc set and the stretching lineation on it

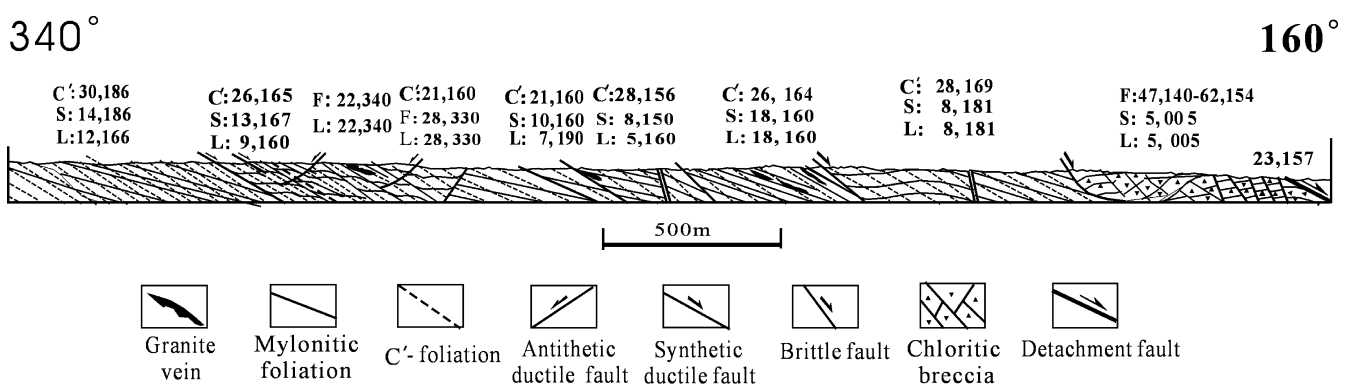

Fig. 7. The Shuiquangou (Spring Valley) cross-section on the southern flank of the Yagan-Onch Hayrhan metamorphic core complex. See Fig. 6 for location.

(53 measurements) have an average dip and dip direction of 24 and 165°. The facts that the ecc set deflect or cut the mylonitic foliation and the lineation on the ecc surface plunges in the same direction but more steeply than the lineation on the mylonitic foliation imply that they belong to the same progressive deformation and that the ecc set formed relatively later.

The antithetic ecc set is not well developed and only eight measurements were obtained. One example is conjugate to a synthetic set with a conjugate angle of 128°; the synthetic ecc has a dip and dip direction of 21 to 165° and antithetic one has a dip and dip direction of 31 to 345° (Fig. 2C). Another conjugate angle is 107° with the synthetic set dipping at 28 to 169° and the antithetic ecc at 45 to 345°.

4.3. Fractures and faults related to the synthetic ecc set

Twenty-one fractures or low-angle ductile normal faults on outcrop scales that are parallel with the ecc surfaces were observed (Figs. 2B and 8B). As shown in Fig. 2B, there are three or four discontinuity surfaces or fractures that are parallel with the ecc surface nearby and truncate the sub-horizontal compositional layering and mylonitic foliation with displacements of several centimeters. A larger scale example is shown in Fig. 8A where a ductile low-angle normal fault with a displacement of several meters is formed.

4.4. The master detachment fault

The master detachment, the Hure detachment fault (Zheng et al., 1991, 1996), strikes in an ENE-direction and extends laterally for over 80 km (Zheng et al., 1996; Webb et al., 1999). The outcrop pattern of the master detachment fault is influenced by fold-like primary corrugations in the detachment fault that are oriented parallel to the south-southeast direction of metamorphic core complex extension (Fig. 6). The fault surface is polished and typically dips to 165° at 22–26°. Six measurements near the section and six measurements to the east from Mongolia shows slickenlines on the fault surface consistently plunge in a direction of ~165°. Some typical nail-head slickenlines indicate top-to-the-south-southeast relative displacement. The fault surface is directly overlain by an 8-m-thick yellow and brick red clay-rich gouge and underlain by a brown and dark green layer of 60-cm-thick flinty microbreccia (Fig. 8B). Below the microbreccia layer is a 250-m-thick chloritic breccia zone where high-angle normal faults and brittle fractures are well developed (Fig. 7).

4.5. Similarity in geometry and kinematics between the ecc set, low-angle normal faults

The following geometric and kinematic relationships can be inferred from the above observations: (a) the mylonitic foliation, the synthetic ecc set and low-angle normal faults in the section dip in about the same direction but the former more gently (~18°) than the latter two; (b) the stretching lineation in the mylonitic foliation and that on the synthetic ecc set, and the slickenlines on the master detachment fault plunge to ~165° but the former at lower angle than the latter two: (c) the synthetic ecc set, synthetic outcrop-scale low-angle normal faults and the master detachment fault share the same attitude and shear sense; (d) antithetic ecc set and antithetic low-angle normal faults have the same attitude and shear sense; (e) the angle of conjugate ecc sets is about 70 or 110° with a bisectrix of the obtuse angle in the sub-vertical contractional direction.

As shown in Fig. 9 in detail, the poles of eccs, synthetic and antithetic ductile normal faults, and mylonitic foliation—as well as stretching lineation and slickenlines on the faults in the Yagan-Onch Hayrhan metamorphic core complex—are all located along a great circle. We interpret these features as representing progressive stages during extreme extension along a SSE-direction in Late Jurassic or Early Cretaceous. The similarity in geometry and kinematics between the ecc set and low-angle normal faults on different scales brings us to the conclusion that the process of low-angle normal fault's formation may extrapolate from micro- to macroscale.

5. Discussion—the formation of low-angle normal faults

5.1. Localization of strain and strain-softening in ecc

As shown in Fig. 2, the mylonitic fabric in the eccs is much stronger than that in the adjoining mylonitic rocks. This implies that high finite strain values are localized in the eccs and that material in the ecc must be softer than the wall rocks. Apparently, changes occur in the rheology of material in the eccs after its nucleation. This effect is known as strain softening. The most important mechanisms that may contribute to softening are (White, 1979; White et al., 1980; Tullis, 1990): (1) a decrease in grain size; (2) grain boundary migration re-crystallization; (3) growth of new minerals (reaction softening); (4) development of a lattice-preferred orientation which places them in a position for easy dislocation glide (geometric softening); (5) enhanced pressure solution due to decrease in grain size and opening of voids and cracks; and (6) 'hydrolytic' weakening of minerals due to diffusion of water into the lattice. In the Yagan metamorphic core complex, a decrease in grain size within the ecc is notable even in hand samples and in outcrop (Fig. 2), the replacement of feldspars by aggregates of white mica and quartz represents growth of new minerals, and development of a preferred orientation of mineral grains (quartz ribbons, mica fish and lens-shaped feldspar porphyroclasts) is universal. Each of these

Fig. 8. (A) A low-angle normal fault on outcrop scale in the footwall mylonitic rocks of the Yagan-Onch Hayrhan metamorphic core complex; (B) the master detachment fault of the Yagan-Onch Hayrhan metamorphic core complex above the rock ledge (microbreccia) is statistically parallel to the synthetic ecc set of Fig. 9.

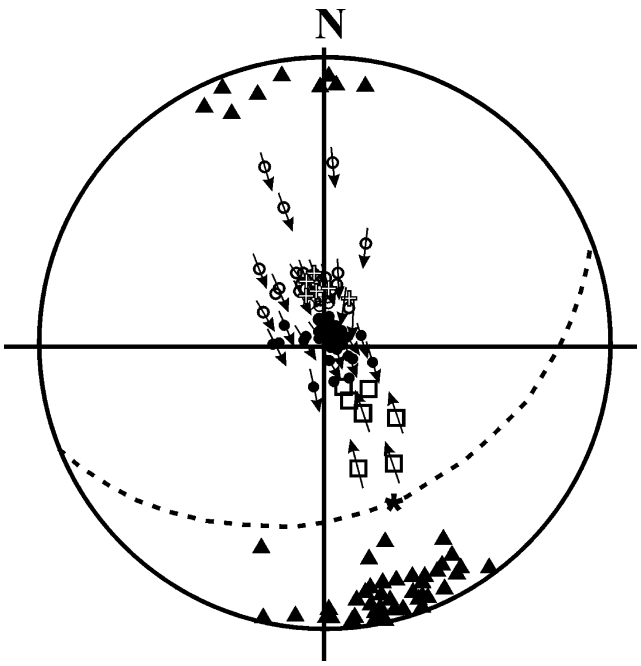

Fig. 9. Lower hemisphere, stereographic projection of poles to synthetic ecc (open circles with an arrow indicating the upper-part-slip direction), synthetic ductile normal faults (open crosses), antithetic ductile normal faults (open squares), the average major detachment fault (the dashed arc) and the average attitude of slickenlines on it (the star), poles to mylonitic foliation (solid circles with an arrow indicating the upper-part-slip direction) and stretching lineations (solid triangles). All measurements are from the southern flank of the Yagan-Onch Hayrhan metamorphic core complex.

mechanisms may, more and less, contribute to the softening of the ecc.

5.2. Translation of the ecc into low-angle normal faults

With progressive deformation, the material bands within eccs become more stretched in the elongation direction and contracted in the normal direction. The cleavage may stop developing when the differential stress reduces below the strength or it may become a low-angle normal fault through strain softening in the shear bands where the stress exceeds the yield strength of the material in the bands. The similarity in geometry and kinematics between the ecc set, low-angle normal faults in the Yagan-Onch Hayrhan metamorphic core complex provides strong evidence for the above interpretation. Single set or conjugate low-angle normal faults are commonly shown in deep seismic reflection profiles recorded in extensional regions, e.g. fig. 3 in Malavieille (1993) and fig.11 in Reston (1990), which may represent the large-scale propagation of eccs. The low angular relationship between the Whipple detachment fault, California and the mylonitic front in its footwall (Davis and Lister, 1988) can be interpreted as an expression of the detachment fault propagating upward out of the mid-crustal mylonitic shear zone along a master ecc surface. In the Hohhot metamorphic core complex of the Daqing Shan (Mountains) of Inner Mongolia (Darby et al., 2001), the low-angle ($<30°$) Hohhot detachment overlies footwall mylonite rocks for a distance of more than 70 km along its strike (at high angle to the direction of extension), the detachment fault is parallel to the synthetic ecc set in the footwall mylonitic rocks (Wang et al., 2002b) and the cut-off angle between the detachment fault and the mylonitic foliation is $\sim 25-30°$ (Davis et al., 2002). These geologic relationships also support our interpretation.

5.3. Propagation and reactivation of low-angle normal faults in brittle domains

The problem is that some low-angle normal faults are without clear relationships to ductile shearing, such as the active Altoberina low-angle normal fault of central Italy (Boncio et al., 2000) and the Miocene Chemehuevi detachment of the Colorado River extensional terrane (John and Foster, 1993). It is necessary to explain the formation of these low-angle normal faults in brittle domains. A similar situation occurs in eastern areas of the Hohhot metamorphic core complex where the detachment fault passes laterally into structurally higher, non-mylonitic footwall rocks without a change in its low angle of dip. It brings us to assume that those low-angle normal faults without footwall mylonitic rocks might have tip lines of mylonitic fronts at depth. This implies that low-angle normal faults could occur in brittle domains through propagation of the eccs in mylonitic rocks.

As extension progresses in a metamorphic core complex, the mylonitic rocks are drawn upwards and out from beneath the developing master ecc surface and into the brittle domain. Once the developing master ecc enters the brittle domain, the maximum shear stresses will develop near their tip lines. Chinnery (1966) analyzed maximum shear stress trajectories near the tips of a strike-slip fault when an increment of movement occurs on the master fault subjected to pure shear and to uniaxial compression. The results of his two analyses show that the maximum stresses are localized at the tips of the master fault and that the master fault will most likely continue to propagate without changing its orientation. As exceptionally weak surfaces, it is reasonable to infer that a certain ecc surface similar to Chinnery's master fault will propagate without changing its orientation. The master ecc may propagate upwards into the brittle domain as a detachment fault. An updated compilation of dip estimates given by Collettini and Sibson (2001) from focal mechanisms of shallow, intracontinental, normal-slip earthquakes shows that the dip distribution extends from 65 to 30° with apparent lockup at $\sim 30°$, for the reactivation angle between the fault and inferred horizontal σ_3. Fault-localized fluid overpressuring, however, may cause less favorable dip angle ($<30°$) faults to reactivate (Sibson, 2000; Collettini and Sibson, 2001).

5.4. Proposed conceptual model for the low-angle normal faults

Once an ecc set has formed in a ductile shear zone, large strains can concentrate in these bands because of softening, and a master ecc surface of these exceptionally weak surfaces becomes a potential low-angle normal fault in the shear zone (Fig. 10A). In our conceptual model, as extension progresses in a metamorphic core complex, the mylonitic rocks are drawn upwards and out from beneath the developing low-angle normal fault and into the brittle domain. Once the developing fault enters the brittle domain, due to stress localization near its tip line, it propagates upwards in a brittle way without changing its orientation (Fig. 10B). At progressively higher, colder levels the mylonitic footwall rocks of the metamorphic core complex are retrograded, and the uplifted part of the master ecc surface now becomes a detachment fault, but likely retains its low-angle attitude beneath the upper-plate rocks if not flattened due to back rotation or doming. The elevated preexisting mechanically weak surface in brittle domains is obviously favorable to frictional slip (Fig. 10C). The progressive downward flattening of the detachment fault implies that the geometry of the lower part of the low-angle normal faults that remains in the lower crust is controlled by plastic laminar flow.

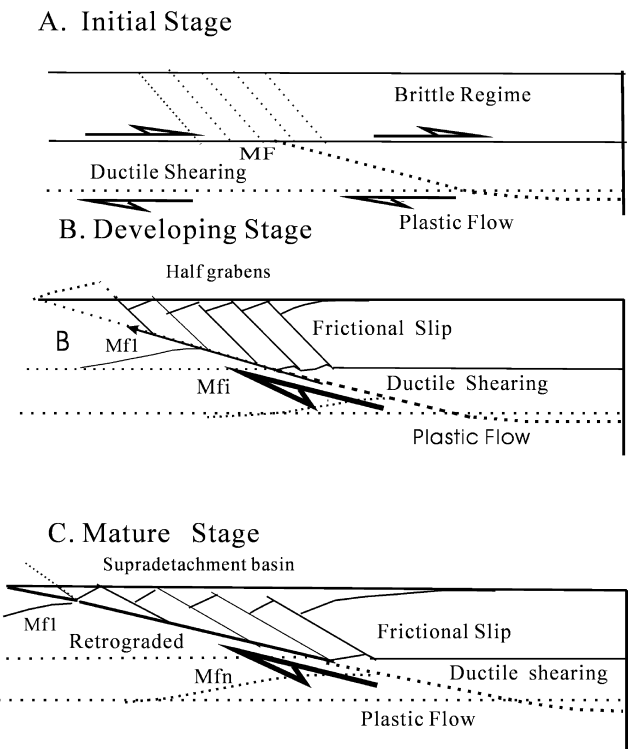

Fig. 10. Upward propagation of a master ecc to form a detachment fault. (A) Initial stage: ductile (mylonitic) shear in a subhorizontal zone related to brittle-ductile transition in middle crust. MF = mylonitic front, the upper limit of mylonitic shear fabric development. The ductile shear zone has not yet generated an upward propagating detachment fault (dotted line). (B) Master fault propagates upwards out of ductile shear zone into brittle crust. Brittle extension of the hanging wall produces an array of synthetic normal faults bounding half grabens. The now inactive MF_1 is transported upwards in the footwall of the detachment fault and a new mylonitic front (MF_i) develops in the uplifting footwall. (C) Mature stage: a succession of new mylonitic fronts (MF_n) develops progressively downwards in the uplifting footwall and a supradetachment basin may develop in the hanging wall.

6. Conclusions

The predicted attitude of faults in elastic model stress fields is based on the Coulomb–Mohr brittle failure criterion with a ~30° angle of internal friction. If correct, the measured angle between conjugate fracture sets should be ~60°, which is not compatible with observations in ductile shear zones. Thus, frictional failure criteria are not applicable to the mechanics of ductile shear in the mid- to lower crust. However, extensional crenulation cleavages (eccs) in ductile shear zones appear, upon applying the effective moment criterion developed here, to be analogous to normal faults in the brittle domains. It is proposed that some ecc sets within shallowly dipping ductile (mylonitic) shear zones can propagate upwards into low-angle extensional faults, any one of which might evolve into a master low-angle normal (detachment) fault. This analysis is supported by the fact that the conjugate angle between ecc sets containing the shortening or σ_1 direction is ~110°. Since the inferred σ_1 is typically sub-vertical in extensional regimes, it is reasonable to suggest that some master low-angle normal faults may result from the upward propagation of a major ecc by strain localization and strain softening. Propagation of the synthetic set of ecc (C′) into low-angle detachment faults is mechanically feasible and offers a new explanation for such faults that reflects the ductile regime in which they are generated. Low-angle normal faults without clear relationships to ductile shearing may be the result of upward propagation of the master ecc due to stress concentration at its upper tip that is still located at depth.

Acknowledgements

NNSFC (Grant No. 40272084) and U.S. NSF (Grant EAR-9903012) support this work. We highly appreciate Dr Tikoff for greatly improving the manuscript; his suggestions were particularly useful in developing our ideas. The writers are grateful to S. Wallis, M. Markley, L. Goodwin and an anonymous reviewer for criticism of the manuscript at various stages in its preparation. Brian Darby, U.S.C., read the manuscript and contributed to its clarity. We also thank Yin An, Cai Yongen and Wang Shimin for helpful discussions. Special thanks due to the editor, Professor Fisher, for his encouragement, thorough and constructive reviews.

References

Abers, G.A., 1991. Possible seismogenic shallow-dipping normal faults in the Woodlark-D'Entrecasteaux extensional province, Papua New Guinea. Geology 19, 1205–1208.

Anderson, E.M., 1951. The Dynamics of Faulting, 2nd ed, Oliver and Boyd, Edinburgh.

Anderson, T.B., 1964. Kink-band and related geological structures. Nature 202, 272–274.

Anderson, T.B., 1974. The relationship between kink-bands and shear fractures in the experimental deformation of slate. Journal of the Geological Society of London 130, 367–382.

Argles, T.W., Platt, J.P., Waters, D.J., 1999. Attenuation and excision of a crustal section during extensional exhumation: the Carratraca Massif, Betic Cordillera, southern Spain. Journal of the Geological Society 156, 149–162.

Becker, G.F., 1893. Finite homogeneous strain, flow and rupture of rocks. Geological Society of America Bulletin 4, 13–19.

Bergh, S.G., Karlstrom, K.E., 1992. The Chaparral shear zone—deformation partitioning and heterogeneous bulk crustal shortening during Proterozoic orogeny in central Arizona. Geological Society of America Bulletin 104, 329–345.

Berthe, D., Choukroune, P., Jegouzo, P., 1979. Orthogneiss, mylonite, and noncoaxial deformation of granite: the example of the South Armorican shear zone. Journal of Structural Geology 2, 31–42.

Blenkinsop, T.G., Treloar, P.J., 1995. Geometry, classification and kinematics of S–C and S–C′ fabrics in the Mushandike area, Zimbabwe. Journal of Structural Geology 17, 397–408.

Boncio, P., Brozzetti, F., Lavecchia, G., 2000. Architecture and seismotectonics of a regional low-angle normal fault zone in central Italy. Tectonics 19, 1038–1055.

Buck, W.R., 1990. Comment on Yin A. "Origin of regional, rooted low-angle normal faults: a mechanical model and its tectonic implications". Tectonics 9, 545–546.

Byerlee, J.D., 1978. Friction of rocks. Pure and Application Geophysics 116, 615–626.

Chinnery, M.A., 1966. Secondary faulting. Canadian Journal of Earth Sciences 3, 163–190.

Collettini, C., Sibson, R.H., 2001. Normal faults, normal friction? Geology 29, 927–930.

Cosgrove, J.W., 1976. The formation of crenulation cleavage. Journal of the Geological Society (London) 132, 155–178.

Crittenden, M.D., Jr., Coney, P.J., Davis, G.H. (Eds.), 1980. Cordilleran Metamorphic Core Complexes. Geological Society of America Memoir 153, p. 490.

Darby, B.J., Davis, G.A., Zheng, Y., 2001. Evolving geometry of the Hohhot metamorphic core complex, Inner Mongolia, China. Geological Society of America Abstracts with Programs 33 (3), A-2.

Davis, G.A., Lister, G.S., 1988. Detachment faulting in continental extension: perspectives from the southwestern U.S. Cordillera. Geological Society of America Special Paper 218, 133–159.

Davis, G.A., Qian, X., Zheng, Y., Tong, H., Yu, H., Wang, C., Gehrels, G.E., Shanfiquallah, M., Fryxell, J.E., 1996. Mesozoic deformation and plutonism in the Yunmeng Shan: a Chinese metamorphic core complex north of Beijing, China. In: Yin, A., Harrison, T.M. (Eds.), The Tectonic Evolution of Asia. Cambridge University Press, pp. 253–280.

Davis, G.A., Darby, B.J., Zheng, Y., Spell, T.L., 2002. Geometric and temporal evolution of an extensional detachment fault, Hohhot metamorphic core complex, Inner Mongolia, China. Geology 30, 1003–1006.

Davis, G.H., Coney, P.J., 1979. Geological development of the Cordilleran metamorphic core complexes. Geology 7, 120–124.

Dennis, A.J., Secor, D.T., 1987. A model for the development of crenulations in shear zones with applications from the southern Appalachian Piedmont. Journal of Structural Geology 9, 809–817.

Dewey, J.F., 1965. Nature and origin of kink bands. Tectonophysics 1, 459–494.

Donath, F.A., 1961. Experimental study of shear failure in anisotropic rocks. Geological Society of America Bulletin 72, 985–989.

Donath, F.A., 1964. Strength variation and deformation behavior in anisotropic rocks. In: Donnelly, T.W., (Ed.), Earth Sciences—Problems and Progress in Current Research, University of Chicago Press, Chicago, pp. 83–103.

Donath, F.A., 1968. Experimental study of kink band development in Martinsburg slate. Geological Survey Paper, Canada 68-52, 255–287.

Doser, D.I., 1987. The Ancash, Peru earthquake of 1946 November 10: evidence for low-angle normal faulting in the high Andes of northern Peru. Geophysical Journal of the Royal Astronomical Society 91, 57–71.

Evans, B., Dresden, G., 1991. Deformation of earth materials: six easy pieces. Contributions in Tectonophysics, U.S. National Report to International Union of Geodesy and Geophysics, 1987–1990. American Geophysical Union, pp. 823–843.

Friedman, M., Logan, J.M., 1973. Lüders' bands in experimentally deformed sandstone and limestone. Bulletin of the Geological Society of America 84, 1465–1476.

Gapais, D., White, S.H., 1982. Ductile shear bands in a naturally deformed quartzite. Textures and Microstructures 5, 1–17.

Gay, N.C., Weiss, L.E., 1974. The relationship between principal stress direction and the geometry of kinks in foliated rocks. Tectonophysics 21, 287–300.

Goodwin, L.B., Wllliams, P.F., 1996. Deformation path partitioning within a transpressive shear zone, Marble Cove, Newfoundland. Journal of Structural Geology 18, 975–990.

Halbich, I.M., 1978. Minor structures in gneiss and origin of steep structures in the Okiep Copper District. Geological Society of South Africa, Special Publication 4, No. 18.

Harris, L.B., Cobbold, P.R., 1985. Development of conjugate shear bands during bulk simple shearing. Journal of Structural Geology 7, 37–44.

Hetzel, R., Passchier, C.W., Ring, U., Dora, O.O., 1995. Bivergent extension in orogenic belts—the Menderes Massif (southwestern Turkey). Geology 23, 455–458.

Hill, R., 1950. The Mathematical Theory of Plasticity, Oxford University Press /Clarendon Press, Oxford.

Hobbs, B.E., Means, W.D., Williams, P.F., 1976. An Outline of Structural Geology, John Wiley & Sons, New York.

Hoeppener, R., Brix, M., Volbrecht, A., 1983. Some aspects on the origin of fold-type fabrics—theory, experiments and field applications. Geologische Rundschau 72, 421–450.

John, B.E., Foster, D.A., 1993. Structural and thermal constrains on the initiation angle of detachment faulting in the southern Basin and Range: the Chemehuevi Mountains case study. Geological Society of America Bulletin 105, 1091–1108.

Johnson, A.M., 1977. Styles of Folding—Development in Geotectonics. Amsterdam, 11, 406pp.

Lister, G.S., Davis, G.A., 1989. The origin of metamorphic core complexes and detachment faults formed during Tertiary continental extension in the northern Colorado River region, USA. Journal of Structural Geology 11, 65–94.

Lister, G.S., Banga, G., Feenstra, A., 1984. Metamorphic core complexes of Cordilleran type in the Cyclades, Aegean Sea, Greece. Geology 12, 221–225.

Malavieille, J., 1993. Late orogenic extension in mountain belts: insights from the Basin and Range and the late Paleozoic Variscan belt. Tectonics 12, 1115–1130.

Mamtani, M.A., Karanth, R.V., 1996. Microstructural evidence for the formation of crenulation cleavage in rocks. Current Science 71, 236–240.

Park, R.G., 1981. Shear-zone deformation and bulk strain in granite-greenstone terrain of the Western Superior Provinces, Canada. Precambrian Research 14, 31–47.

Passchier, C.W., 1991. Geometric constrains on the development of shear bands in rocks. Geologie en Mijnbouw 70, 203–211.
Passchier, C.W., 2001. Flanking structures. Journal Structural Geology 23, 951–962.
Passchier, C.W., Trouw, R.A., 1996. Microtectonics, Springer-Verlag, Heidelberg, Berlin.
Paterson, M.S., Weiss, L.E., 1966. Experimental deformation and folding in phyllite. Geological Society of America Bulletin 77, 343–374.
Platt, J.P., 1979. Extensional crenulation cleavage. Journal Structural Geology 1, 95.
Platt, J.P., 1984. Secondary cleavages in ductile shear zones. Journal of Structural Geology 6, 439–442.
Platt, J.P., Vissers, R.L.M., 1980. Extensional structures in anisotropic rocks. Journal of Structural Geology 2, 397–410.
Price, N.J., Cosgrove, J.W., 1990. Analysis of Geological Structures, Cambridge University Press, Cambridge, UK, 502pp.
Reston, T.J., 1990. The lower crust and the extension of the continental lithosphere: kinematic analysis of BIRPS deep seismic data. Tectonics 9, 1235–1248.
Shea, W.T. Jr, Kronenberg, A.K., 1993. Strength and anisotropy of foliated rocks with varied mica contents. Journal of Structural Geology 15, 1097–1121.
Sibson, R.H., 2000. Fluid involvement in normal faulting. Journal of Geodynamics 29, 469–499.
Simpson, C., De Paor, D.G., 1993. Strain and kinematic analysis in general shear zones. Journal of Structural Geology 15, 1–20.
Sorel, D., 2000. A Pleistocene and still-active detachment fault and the origin of the Corinth–Patras rift, Greece. Geology 28, 83–86.
Tchalenko, J.S., 1968. The evolution of kink bands and the development of compression textures in sheared clay. Tectonophysics 6, 159–174.
Tullis, J., 1990. Experiment studies of deformation mechanisms and microstructures in quartzo-feldspathic rocks. In: Barber, D.J., Meredith, P.G. (Eds.), Deformation Processes in Minerals, Ceramics and Rocks, Unwin Hyman, London, UK, pp. 190–227.
Wang, T., Zheng, Y., Li, T., Gao, Y., Ma, M., 2002a. Forceful emplacement of granitic plutons in an extensional tectonic setting: syn-kinematic plutons in the Yagan-Onch Hayrhan Metamorphic core complex. Acta Geologica Sinica 76, 81–88.
Wang, X., Zheng, Y., Zhang, J., Davis, G.A., Darby, B.J., 2002b. Extensional kinematic characteristics and shear type of Huhhot metamorphic core complex, Inner Mongolia, China. Geological Bulletin of China 21, 238–243.(in Chinese with English abstract).
Watterson, J., 1999. The future of failure: stress or strain? Journal of Structural Geology 21, 939–948.
Webb, L.E., Graham, S.A., Johnson, C.L., Badarch, B., Hendrix, M.S., 1999. Occurrence, age, and implications of the Yagan-Onch Hayrhan metamorphic core complex, southern Mongolia. Geology 27, 143–146.
Weijermars, R., 1993. Progressive deformation of single layers under constantly oriented boundary stresses. Journal of Structural Geology 15, 911–922.
Weijermars, R., 1998. Taylor-mill analogues for patterns of flow and deformation in rocks. Journal of Structural Geology 20, 77–92.
Weiss, L.E., 1968. Flexural slip folding of foliated model materials. In: Baer, A J., Norris, D.K. (Eds.), Proceedings Conference on Research in Tectonics. Canada Geological Survey, Ottawa. Paper 68-52.
Weiss, L.E., 1980. Nucleation and growth of kink bands. Tectonophysics 65, 1–38.
Wernicke, B., 1981. Low-angle normal faults in the Basin and Range province—Nappe tectonics in an extending orogen. Nature 291, 645–648.
Westaway, R., 1999. The mechanical feasibility of low-angle normal faulting. Tectonophysics 308, 407–443.
White, S.H., 1979. Large strain deformation: report on a Tectonic Studies Group discussion meeting held at Imperial College, London on 14 November 1979. Journal of Structural Geology 1, 333–339.
White, S.H., Burrows, S.E., Carreras, J., Shaw, N.D., Humphreys, F.J., 1980. On mylonites in ductile shear zones. Journal Structural Geology 2, 175–187.
Williams, P.F., Price, G., 1990. Origin of kinkband and shear band cleavage in shear zones: an experimental study. Journal of Structural Geology 12, 145–164.
Wills, S., Buck, W.R., 1997. Stress-field rotation and rooted detachment faults: a Coulomb failure analysis. Journal of Geophysical Research 102, 20503–20514.
Yin, A., 1989. Origin of regional, rooted low-angle normal faults: a mechanical model and its tectonic implications. Tectonics 8, 469–482.
Zhang, J., Zheng, Y., Liu, S., 1998. The Xiaoqinling Metamorphic Core Complex: Structures, Mechanisms and Evolution, Oceanic Publishing House, Beijing, (in Chinese).
Zheng, Y., 1992. A quantitative analysis of the angle between conjugate sets of extensional crenulation cleavages: an explanation of the low-angle-normal-fault development. Abstracts, 3-1, 131 of 29th IGC, Kyoto, Japan.
Zheng, Y., Du, S., 1985. A Quantitative Analysis of the Angle Between Conjugate Kink Bands: Scientific Papers on Geology for International Exchange 2, pp. 175–180. Geological Publishing House, Beijing.
Zheng, Y., Zhang, Q., 1994. The Yagan metamorphic core complex and extensional detachment fault in Inner Mongolia, China. Acta Geologica Sinica 7, 125–135.
Zheng, Y., Wang, S.Z., Wang, Y.F., 1991. An enormous thrust nappe and extensional metamorphic core complex newly discovered in Sino-Mongolian boundary area. Science in China 34, 1145–1154.
Zheng, Y., Zhang, Q., Wang, Y, Liu, R., Wang, S.G., Zuo, G., Wang, S.Z., Lkaasuren, B., Badarch, G., Badamgarav, Z., 1996. Great Jurassic thrust sheets in Beishan (North Mountains)–Gobi areas of China and southern Mongolia. Journal of Structural Geology 18, 1111–1126.